

Testing Gravity with Pulsar Scintillation Measurements

Huan Yang,^{1,2} Atsushi Nishizawa,^{3,4} and Ue-Li Pen^{1,5,6,7}

¹*Perimeter Institute for Theoretical Physics, Waterloo, ON N2L2Y5, Canada*

²*Institute for Quantum Computing, University of Waterloo, Waterloo, ON N2L3G1, Canada*

³*Department of Physics and Astronomy, The University of Mississippi, University, MS 38677, USA*

⁴*Theoretical Astrophysics 350-17, California Institute of Technology, Pasadena, California 91125, USA*

⁵*Canadian Institute for Theoretical Astrophysics,
60 St. George Street, Toronto, On M5S3H8, Canada*

⁶*Canadian Institute for Advanced Research, CIFAR program in Gravitation and Cosmology*

⁷*Dunlap Institute for Astronomy & Astrophysics, University of Toronto,*

AB 120-50 St. George Street, Toronto, ON M5S 3H4, Canada

(Dated: February 27, 2018)

We propose to use pulsar scintillation measurements to test predictions of alternative theories of gravity. Comparing to single-path pulsar timing measurements, the scintillation measurements can achieve a part in a thousand accuracy within one wave period, which means pico-second scale resolution in time, due to the effect of multi-path interference. Previous scintillation measurements of PSR B0834+06 have data acquisition for hours, making this approach sensitive to mHz gravitational waves. Therefore it has unique advantages in measuring gravitational effect or other mechanisms on light propagation. We illustrate its application in constraining scalar gravitational-wave background, in which case the sensitivities can be greatly improved with respect to previous limits. We expect much broader applications in testing gravity with existing and future pulsar scintillation observations.

I. INTRODUCTION

Pulsar scintillation happens when pulsed radio signals from pulsars follow different paths of propagation to reach the Earth, and exists for almost all known pulsars. It is generally known that structures in interstellar plasma along the propagation path plays the role of an effective “lens” and generates necessary lensing for pulses along different paths to meet at the Earth. Upon arrivals, these radio signals interfere with each other and generate a spatially and frequency varying interference pattern. As the Earth is moving, an telescope observer experiences time-dependent intensity variation corresponding to different fringes in the interference pattern. The nature of these lenses is not fully understood, but appears to be dominated by rare, isolated coherent plasma structures. Quantitative models have been proposed to provide precision templates using a small number of optical caustic parameters[1, 2].

As the illustration in Fig. 1, the spatial separation between fringes is approximately λ_e/α (λ_e is the radio wavelength, α is the path opening angle) and the temporal separation is $\sim \lambda_e/(\alpha V_e)$, where V_e is the projected Earth-lens-pulsar velocity, generally dominated by the pulsar proper velocity. With α assumed to be \sim arcsec, one typically observes a scintillation time scale of seconds, typically longer than the pulsar period. By statistically (see the discussion in the next section) averaging over time shift of the fringes, it is possible to achieve phase accuracy that is equivalent to pico-second resolution in time. This is a factor of 10^5 higher than the accuracy in single-path pulsar timing [3]. It is worth to note, however, scintillation measurement is fundamentally different from traditional pulsar timing measure-

ments, where the relevant physical quantity in the formal scenario is the radio wave phase differences, and in the latter case it is the pulse arriving time. Therefore it is important to bear in mind that the “timing precision” in this paper actually refers to the phase accuracies in phase.

This unprecedented phase accuracy (and equivalent timing precision) allows one to apply the scintillation to probing the physics of plasma structures in an interstellar medium [4, 5] and constraining the size of emission regions in the pulsar magnetospheres [6]. Although high-precision pulsar timing has been discussed extensively in literature to test alternative theories of gravity, little was known in relating scintillation measurements to testing gravity. In this paper, we propose to use pulsar scintillation measurements as a laboratory for gravitational physics, in particular, as a detector of scalar gravitational waves (GWs), which appear in alternative theory of gravity. Similar analysis can be applied to test other physical effects that affect the propagation of radio waves.

A. Scintillation Modulation

Propagating gravitational distortions modulate the plasma lensing effects. The plasma lenses can change shape on a sound crossing time, which is typically four orders of magnitude longer than the gravitational time scales. This allows precise measurements of space-time variations that are unlikely to be mimicked by plasma effects. If there exists the GW large enough to be detected, it would lead to an irreducible scintillation model residual.

In the absence of GWs, the variation of the plasma

propagation Green's function is dominated by the Earth-lens-pulsar relative motion. Interstellar holography retrieves the time dependent Green's functions, and has been demonstrated to reproduce observed scintillation patterns to parts per million [7]. These authors are able to decompose the dynamic spectrum as a sum of Green's functions kernel lying approximately on a parabolic set of loci. These lenses are located at a distance of 389pc from earth, with a pulsar distance of 640pc[2]. The parabolic relationship arises from the collinearity of lensing points: the time delay through is lens is proportionate to the square of its transverse separation angle. The doppler frequency is the time derivative of this delay due to the pulsar's apparent motion relative to the screen, and is linear in transverse separation, thus resulting in a parabolic relationship of delay and doppler rate of the lensing images. As a result, plasma lensing induces a modulation frequency proportional to image separation, whereas the change induced by GWs is independent of the separation. Such a pattern is not observed. We interpret that achieved dynamic range of 63dB that no modulation of more than a part in a thousand in the dynamic spectrum can be due to gravitational waves moving at the speed of light. The observing frequency was approximately 300 MHz, corresponding to wave period $\sim 3\text{ns}$ and a Nyquist voltage sampling rate of 1.5ns. We thus estimate the maximum contribution of gravitational waves at most a part per thousand, or about a picosecond as the limit on the allowed inverse delay-doppler power. The lower bound of measurable frequency is constraint by the total observation time t_{obs} (for the work in [7], $1/t_{\text{obs}} \sim \text{mHz}$). The upper bound of frequency is related to the separation between pulses $1/t_{\text{sep}}$, as the pulse sequence determines a natural sampling frequency. A more precise analysis would require access to the data and holography algorithm.

The accuracy of this model is limited only by thermal noise, and not by pulsar self-noise. A typical $\Delta t \sim \text{hour}$ long observation with $\Delta\nu \sim 100 \text{ MHz}$ bandwidth leads to a flux uncertainty of $\text{SEFD}/\sqrt{\Delta t \delta\nu}$, where SEFD is the system equivalent flux density. For large telescopes such as FAST or Arecibo, SEFD is about 5 Jy. There are further subtleties which could affect the sensitivity of scintillation measurement for gravitational waves. First, the 63dB in power or factor of 10^3 in signal-to noise-ratio (SNR) is achieved mainly near the bottom of the parabola in the decay time-doppler shift curve, where the signal is the strongest and the effect of GW vanishes. At larger opening angle the data could encode the information GWs but the SNR is lower. Therefore for each specific data set one should try to find the optimum opening delay that balances these two effects. Secondly, it is possible that following the treatment in [7], part of the noise is absorbed in the model. Therefore it is unclear what fraction of the GW power remains in the residuals. Such fraction may also vary depending on the types of GWs: i.e., single source, continuous/burst sources, GW background, etc.

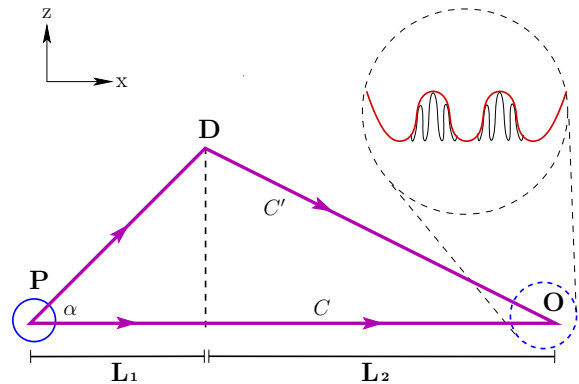


FIG. 1: (Color Online). The illustration for pulsed signals that arrive on the Earth following two distinctive paths, where the wave following C' is deflected by the interstellar medium at location "D". Here $L_1 = r/(1+r)L$ and $L_2 = L/(1+r)$. When the radio waves from these two directions reach the observer on the Earth, they interfere and produce very fine interference pattern based on the radio wavelength λ_e and the path opening angle α . As the Earth moves at a speed $V_e \sim 30 \text{ km/s}$, there are many fringes within the timescale of a single pulse (for illustration purpose we only show a few fringes within each pulse).

II. PROBING NONTENSORIAL COMPONENTS OF GWS

According to the theory of General Relativity, GWs have only two tensor polarizations that are transverse to the wave propagation direction. However, in general metric theory of gravitation [8], since the metric perturbation $h_{\mu\nu}$ has 10 components, 4 of which are purely gauge and eliminated by imposing the condition $h_{0\mu} = 0$, there are 6 degrees of freedom left in h_{ij} ($1 \leq i, j \leq 3$). Therefore gravitational wave emissions with scalar and vector polarizations are predicted in many alternative theories of gravity, such as scalar-tensor theory, $f(R)$ theory, bimetric theory, etc. (For the summary about GW polarization prediction in various alternative gravity models, see [9] and reference therein). Measuring and/or constraining GWs with nontensorial polarizations are a viable approach to test the theories of gravity and search for possible new physics.

We follow the convention in [9, 10] to label these 6 polarizations (2 tensor modes: + and \times , 2 vector modes: x and y , and 2 scalar modes: b , l). In the case that GW

is propagating along z -axis, the tensor bases are

$$\begin{aligned}\tilde{e}^+ &= \begin{pmatrix} 1 & 0 & 0 \\ 0 & -1 & 0 \\ 0 & 0 & 0 \end{pmatrix}, & \tilde{e}^x &= \begin{pmatrix} 0 & 1 & 0 \\ 1 & 0 & 0 \\ 0 & 0 & 0 \end{pmatrix}, \\ \tilde{e}^b &= \begin{pmatrix} 1 & 0 & 0 \\ 0 & 1 & 0 \\ 0 & 0 & 0 \end{pmatrix}, & \tilde{e}^l &= \begin{pmatrix} 0 & 0 & 0 \\ 0 & 0 & 0 \\ 0 & 0 & 1 \end{pmatrix}, \\ \tilde{e}^x &= \begin{pmatrix} 0 & 0 & 1 \\ 0 & 0 & 0 \\ 1 & 0 & 0 \end{pmatrix}, & \tilde{e}^y &= \begin{pmatrix} 0 & 0 & 0 \\ 0 & 0 & 1 \\ 0 & 1 & 0 \end{pmatrix},\end{aligned}\quad (1)$$

so that h_{ij} can be decomposed as

$$h_{ij} = \sum_A h_A \tilde{e}_{ij}^A. \quad (2)$$

As an illustration for applications of pulsar scintillation observations to testing gravity, we show that the existing data provide the best constraint on scalar GWB at mHz band, which beats the previous constraint by four orders of magnitude and might be improved by future space-based GW missions such as eLISA [11].

As shown in Fig. 1, we consider a train of radio waves emitted from Pulsar (“P”) propagates along two different paths (\mathcal{C} and \mathcal{C}') and eventually reaches the Earth. For simplicity, we consider only one-time deflection by the turbulent plasma at location “D” (which is straightforward to generalize to cases with multiple deflections), and assume both paths are on the $x-z$ plane, with \mathcal{C} being along x axis. The coordinate of “P”, “D”, and “O”

on the $x-z$ plane is $[0, 0]$, $[Lr/(1+r), Lr\alpha/(1+r)]$, $[L, 0]$ respectively, where $r \equiv L_1/L_2$ in Fig. 1.

In order to obtain the sensitivity curve to GWs, we derive the transfer functions from GWs with frequency ω_g in such a system. Based on the standard pulsar timing analysis, the GW-induced phase shift of radio waves propagating along \mathcal{C} is (hereafter we adopt the geometric unit that the speed of light $c = 1$)

$$H_C = \frac{\pi n^i h_{ij} n^j \sin[\omega_g L \xi + \psi] - \sin \psi}{\omega_g \lambda_e \xi}, \quad (3)$$

where ψ is the initial phase of that particular GW, $\xi \equiv 1 - \mathbf{k} \cdot \mathbf{n}$, with \mathbf{k} being the unit direction vector of the GW and $\mathbf{n} = \mathbf{e}_x$ being the unit direction vector of $P \rightarrow O$.

Following the same principle, the phase shift (due to the same GW train) of radio waves propagating along \mathcal{C}' is

$$\begin{aligned}H_{C'} &= \frac{\pi n_1^i h_{ij} n_1^j \sin[\omega_g r L \xi_1 + \psi] - \sin \psi}{\omega_g \lambda_e \xi_1} \\ &+ \frac{\pi n_2^i h_{ij} n_2^j \sin[\omega_g L \xi + \psi] - \sin[\omega_g r L \xi_1 + \psi]}{\omega_g \lambda_e \xi_2},\end{aligned}\quad (4)$$

where $\mathbf{n}_1 = \mathbf{e}_x + \alpha \mathbf{e}_z$, $\mathbf{n}_2 = \mathbf{e}_x - r\alpha \mathbf{e}_z$ and $\xi_{1,2} = 1 - \mathbf{n}_{1,2} \cdot \mathbf{k}$. With H_C and $H_{C'}$, we can derive the phase shift after averaging over sky directions of the GWs and their initial phases. For example, considering the longitudinal mode, we have

$$\begin{aligned}H_{C'} - H_C &= \frac{\pi h_l}{\omega_g \lambda_e} \left\{ (\sin[\omega_g L_1 (1 - \mathbf{n}_1 \cdot \mathbf{k}) + \psi] - \sin \psi) \left(\frac{1}{1 - \mathbf{n}_1 \cdot \mathbf{k}} - \frac{1}{1 - \mathbf{n}_2 \cdot \mathbf{k}} \right) \right. \\ &\quad \left. + (\sin[\omega_g L (1 - \mathbf{k} \cdot \mathbf{n}) + \psi] - \sin \psi) \left(\frac{1}{1 - \mathbf{n}_2 \cdot \mathbf{k}} - \frac{1}{1 - \mathbf{k} \cdot \mathbf{n}} \right) \right\}.\end{aligned}\quad (5)$$

The expression of $(H_{C'} - H_C)^2$ follows obviously. After averaging over the random initial phase ψ , and then perform an average over the azimuthal angle around n direction, we arrive at

$$(H_{C'} - H_C)^2 \approx \frac{\pi^2 h_l^2 \alpha^2 (2 - \xi)}{2\omega_g^2 \lambda_e^2 \xi^3} \left\{ (1 - \cos[\omega L_1 \xi]) \frac{1}{1+r} - (1 - \cos[\omega L \xi]) \frac{r}{(1+r)^2} + (1 - \cos[\omega L_2 \xi]) \frac{r}{1+r} \right\}. \quad (6)$$

At last the above expression is averaged for ξ (from 0 to 2) and that gives the corresponding $\delta\Phi^2$ or

$$\delta\Phi = \frac{\pi h_l \alpha L}{\lambda_e} \sqrt{\frac{r}{2(1+r)}} \sqrt{\log(1+r) + r \log \frac{1+r}{r}}. \quad (7)$$

In fact, for other polarizations, we can follow similar procedure to compute the transfer functions. Their scal-

ings are like

$$\begin{aligned}\delta\Phi^2 &\equiv \langle (H_C - H_{C'})^2 \rangle \\ &\propto \frac{h_m^2 \alpha^2}{\omega_g^2 \lambda_e^2} \times \begin{cases} \log(\omega_g L), & A = +, \times b, \\ \omega_g L, & A = x, y, \\ \omega_g^2 L^2, & A = l, \end{cases}\end{aligned}\quad (8)$$

assuming $\omega_g L \gg 1$ (at mHz band it is greater than 10^8

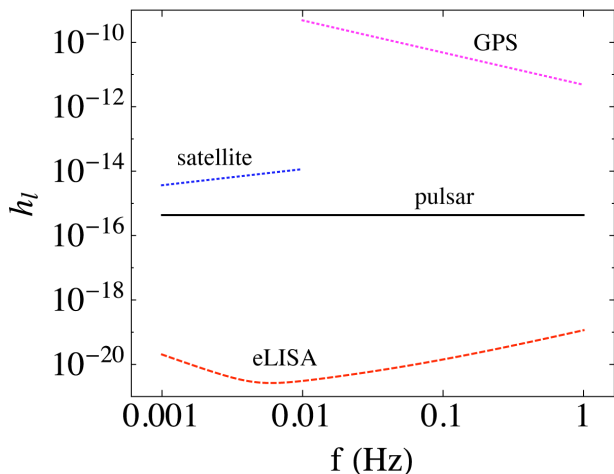


FIG. 2: (Color Online). The constraint on dimensionless amplitude of longitudinal scalar GWs. The lines correspond to sensitivity curves given by previous Doppler tracking of spacecraft [12, 13] (blue dotted), GPS satellites [14] (magenta dotted), pulsar scintillation from PSR B0834+06 ($r \sim 0.64$, $\alpha \sim 20\text{mas}/r \sim 31\text{mas}$, and $L \sim 640\text{pc}$ [2, 15], black solid), and future eLISA measurements (red dashed), respectively. Notice that with the triangular geometry of eLISA, it is difficult to separate out different polarizations of GWs.

for typical pulsars). In particular, we find that the longitudinal mode (“ l ”) receives the largest amplification factor ($\propto \omega_g^2 L^2$), while the amplitudes of all other polarizations are suppressed due to the transverse nature of GW propagation. From this reason, here we focus on the longitudinal mode.

Combining the longitudinal transfer function with the timing noise estimate given in the previous section, we can obtain the sensitivity of pulsar scintillation measurement on longitudinal scalar GWs, by making $\delta\Phi = 2\pi c\delta t_f/\lambda_e$. Take $r \sim 1$, this gives the sensitivity on h_l (dimensionless GW amplitude) as

$$h_l = 6.8 \times 10^{-18} \frac{\delta t_{\text{mHz}}}{1 \text{ ps}} \left(\frac{\alpha}{\text{arcsec}} \right)^{-1} \left(\frac{L}{\text{kpc}} \right)^{-1}. \quad (9)$$

In Fig. 2, we compare the sensitivity to longitudinal scalar GWs based on scintillation measurements of PSR B0834+06 (from [7, 15]) with the current best constraint from Doppler tracking of the *Cassini* spacecraft in [12, 13] and timing measurement of the GPS system in [14] and the proposed sensitivity of eLISA at the same frequency band. As discussed earlier, the SNR of scintillation measurement varies for different opening angle, and in practise the optimal opening angle could be different from the 25mas limit obtained in [15]. These sensitivities are computed by considering the transfer functions of the scalar longitudinal mode, which give approximately the same responses as the tensor mode for Doppler timings and eLISA below 0.1 Hz [16] but better sensitivity of eLISA above 0.1 Hz. We can see that scintillation measurement from PSR B0834+06 already improves the previous sen-

sitivity by a factor of $10 - 10^6$ (greater improvement comparing to the GPS limit). By choosing more distant pulsars, larger opening angles, and/or the ones with better scintillation timing accuracy, as well as statistically averaging data for different scintillating pulsars, it is possible to dramatically improve this limit.

III. CONSTRAINT ON SCALAR-TENSOR RATIO OF GWS

It would be convenient to define the ratio of GW amplitude in scalar mode to that in tensor mode as $R_{\text{ST}} \equiv h^S/h^T$ and useful to show the upper limit in terms of R_{ST} . The advantage to use R_{ST} is that it can be interpreted as the relative strength of scalar coupling in a gravity theory to that of the ordinary gravitational (tensor) coupling, because the ratio is irrespective of common factors between the scalar and tensor modes, e.g. distance to the source and the way of propagation in the interstellar space. It should be emphasized that in general in modified gravity theory, the scalar coupling strength depends on an environment in the Universe, so called the screening mechanism, e.g. the Chameleon mechanism, the Vainshtein mechanism, and etc. [17, 18]. Our constraint is obtained in a low-density and weak-gravity region (in cosmological sense). In a high-density and stronger-gravity region such as near a GW source or on the Earth, relatively large deviation from general relativity is allowed where screening mechanism is also likely to operate. However, that part of contribution is highly model-dependent.

To derive the upper limit on R_{ST} , what we need is the upper limit on the scalar amplitude in Eq. (9) and the amplitude in the tensor mode. The latter is source-dependent and has large uncertainty, depending on astrophysical scenarios. Thus we take into account this uncertainty, adopting the lowest, intermediate, and highest event rates among predictions in literature when we derive the power spectrum densities S_h of each GW source. For white dwarf (WD) binaries, the extragalactic component dominates at $f > 1\text{mHz}$ and the spectrum has been estimated in [19] as $S_h^{\text{WD}}(f) = \{0.37, 1.4, 2.3\} \times 10^{-46} (f/\text{Hz})^{-7/3} \exp[-f/0.01\text{Hz}] \text{ Hz}^{-1}$, each corresponding to the lowest, intermediate, and highest event rates. For neutron star (NS) binaries, compiling the present merger rate [20] and its redshift evolution [21] gives $S_h^{\text{NS}}(f) = \{0.016, 1.6, 16\} \times 10^{-47} (f/1\text{Hz})^{-7/3}$ below a kHz band. For black hole (BH) binaries, the recent detection of a massive BH binary indicates that the merger rate of BH binaries may be higher than the previous expectations [22]. Although the power spectrum of the GWB depends on models of BH binary formation, the *fiducial* model in [22] gives $S_h^{\text{BH}}(f) = \{0.86, 4.7, 16\} \times 10^{-47} (f/1\text{Hz})^{-7/3}$ without a high frequency cutoff in our interest frequency band.

In Fig. 3, the constraints on R_{ST} for each GW source

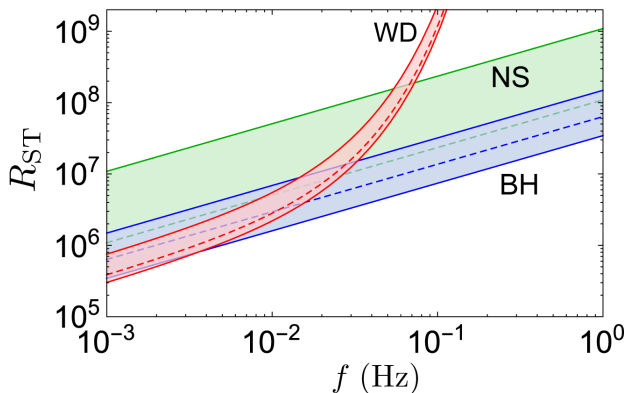


FIG. 3: (Color Online). Upper limit on the scalar-to-tensor ratio R_{ST} for each GWB source with uncertainties of merger rates: WD binaries (red), NS binaries (green), and BH binaries (blue). The dashed lines correspond to the intermediate merger rates and the solid lines are the lowest and highest merger rates.

are shown. The upper bound is tighter at lower frequencies, which are at 1 mHz, 3.9×10^5 , 1.1×10^6 , and 6.4×10^5 for the intermediate merger rates of WD, NS, and BH binaries, respectively. Although the numerical values appear to be much larger than one, they are the first constraints on R_{ST} obtained in the frequency band from 1 mHz to 1 Hz in the low-density and weak-gravity region of space, and they connect the physics of GW emission of a source and a screening mechanism in a model-independent way. There have been the constraints at different frequencies from other observations. The observation of the orbital-period derivative from PSR B1913+16 agrees well with predicted values of GR, conservatively, at a level of 1% error [23]. This fact indicates that the contribution of scalar GWs to the energy loss is less than 1%, that is, $R_{ST} \lesssim 10^{-1}$ at 7.2×10^{-9} Hz at the source position of the NS binary. On the other hand, the recent detection of GWs (GW150914) [24] gives no constraint on the scalar component, as at least three detectors are needed to break the degeneracy of the polarization modes [25].

IV. DISCUSSION AND CONCLUSION

Comparing to single path pulsar timing measurements, the scintillation measurements have better timing accuracies, and the phase-comparison geometry which naturally removes intrinsic noise from the source. These are the key factors which ensures its ultra precision and enables its application to studying ISM physics, pulsar physics, and our proposal in this paper - testing alternative gravity models.

We have illustrated an example in this proposal: measuring a longitudinal scalar GWB. It is also possible to apply to other tests which do not involve GWs - for example, the spacetime quantum fluctuations [26, 27] or the holographic noise [28]. They would contribute distinctive phase noise for photon traveling along different scintillation paths, and hence can be measured by observing anomalous scintillation phase shift or degrading of the interference pattern.

Acknowledgments

The authors appreciate many helpful comments from the referees, especially regarding many aspects of the scintillation discussions. HY thank I-Sheng Yang for very instructive discussions on timing noise of Pulsar scintillations and Nestor Ortiz for making Fig.1. HY acknowledges supports from the Perimeter Institute of Theoretical Physics and the Institute for Quantum Computing. AN are supported by NSF CAREER Grant No. PHY-1055103 and the H2020-MSCA-RISE- 2015 Grant No. StronGrHEP-690904. AN thanks the hospitality of Perimeter Institute, where part of the work was performed. Research at Perimeter Institute is supported by the government of Canada through the Department of Innovation, Science and Economic Development Canada and by the Province of Ontario through Ministry of Research and Innovation.

[1] U.-L. Pen and Y. Levin, *mnras* **442**, 3338 (2014), 1302.1897.
[2] S. Liu, U.-L. Pen, J.-P. Macquart, W. Brisken, and A. Deller, *mnras* **458**, 1289 (2016), 1507.00884.
[3] U.-L. Pen, J.-P. Macquart, A. T. Deller, and W. Brisken, *Mon. Not. R. Astron. Soc.* **440**, L36 (2014), 1301.7505.
[4] B. J. Rickett, *Ann. Rev. Astron. Astrophys.* **15**, 479 (1977).
[5] B. J. Rickett, *Astrophys. J.* **307**, 564 (1986).
[6] C. R. G. M. D. Johnson and P. Demorest, *Astrophys. J.* **758**, 8 (2012).
[7] M. A. Walker, L. V. E. Koopmans, D. R. Stinebring, and

W. van Straten, *Mon. Not. R. Astron. Soc.* **388**, 1214 (2008), 0801.4183.
[8] D. M. Eardley, D. L. Lee, A. P. Lightman, R. V. Wagoner, and C. M. Will, *Phys. Rev. Lett.* **30**, 884 (1973).
[9] A. Nishizawa, A. Taruya, K. Hayama, S. Kawamura, and M. Sakagami, *Phys. Rev. D* **79**, 082002 (2009).
[10] K. J. Lee, *Class. Quantum Grav.* **30**, 224016 (2013).
[11] P. Amaro-Seoane, S. Aoudia, S. Babak, P. Binétruy, E. Berti, A. Bohé, C. Caprini, M. Colpi, N. J. Cornish, K. Danzmann, et al., *GW Notes*, Vol. 6, p. 4-110 **6**, 4 (2013), 1201.3621.
[12] B. Bertotti, R. Ambrosini, J. W. Armstrong, et al., *As-*

- tron. *Astrophys.* **296**, 13 (1995).
- [13] J. W. Armstrong, L. Iess, P. Tortora, and B. Bertotti, *Astrophys. J.* **599**, 806 (2003).
- [14] S. Aoyama, R. Tazai, and K. Ichiki, *Phys. Rev. D* **89**, 067101 (2014).
- [15] W. F. Brisken, J.-P. Macquart, J.-J. Gao, B. Rickett, W. Coles, A. Deller, S. Tingay, and C. West, *The Astrophysical Journal* **708**, 232 (2009).
- [16] M. Tinto and M. E. da Silva Alves, *Phys. Rev. D* **82**, 122003 (2010).
- [17] J. Khoury and A. Weltman, *Phys. Rev. D* **69**, 044026 (2004).
- [18] A. I. Vainshtein, *Phys. Lett. B.* **39**, 393 (1972).
- [19] A. J. Farmer and E. S. Phinney, *Mon. Not. Roy. Astron. Soc.* **346**, 1197 (2003), astro-ph/0304393.
- [20] J. Abadie, B. P. Abbott, R. Abbott, M. Abernathy, T. Accadia, F. Acernese, C. Adams, R. Adhikari, P. Ajith, B. Allen, et al., *Classical and Quantum Gravity* **27**, 173001 (2010), 1003.2480.
- [21] C. Cutler and J. Harms, *Phys. Rev. D* **73**, 042001 (2006), gr-qc/0511092.
- [22] The LIGO Scientific Collaboration and the Virgo Collaboration, ArXiv e-prints (2016), 1602.03847.
- [23] J. M. Weisberg, D. J. Nice, and J. H. Taylor, *Astrophys. J.* **722**, 1030 (2010), 1011.0718.
- [24] B. P. Abbott, R. Abbott, T. D. Abbott, M. R. Abernathy, F. Acernese, K. Ackley, C. Adams, T. Adams, P. Addesso, R. X. Adhikari, et al., *Physical Review Letters* **116**, 061102 (2016), 1602.03837.
- [25] A. Nishizawa, A. Taruya, and S. Kawamura, *Phys. Rev.* **D81**, 104043 (2010), 0911.0525.
- [26] Y. J. Ng and H. van Dam, *Modern Physics Letters A* **9**, 335 (1994).
- [27] G. Amelino-Camelia, *Nature (London)* **398**, 216 (1999), gr-qc/9808029.
- [28] C. J. Hogan, *Phys. Rev. D* **77**, 104031 (2008), 0712.3419.